Superconducting proximity effect on the block antiferromagnetism in $K_yFe_{2-x}Se_2$

Hong-Min Jiang,[1,2] Wei-Qiang Chen,[3,1] Zi-Jian Yao,[1] and Fu-Chun Zhang[1,4]
[1]*Department of Physics and Center of Theoretical and Computational Physics, University of Hong Kong, Hong Kong, China*
[2]*Department of Physics, Hangzhou Normal University, Hangzhou, China*
[3]*Department of Physics, South University of Science and Technology of China, Shenzhen, China*
[4]*Department of Physics, Zhejiang University, Hangzhou, China*
(Received 17 November 2011; revised manuscript received 17 February 2012; published 13 March 2012)

It has been recently discovered that the superconducting (SC) ternary iron selenides have a block antiferromagnetic (AFM) long-range order. Many experiments show a possible mesoscopic phase separation of the superconductivity and antiferromagnetism, while a neutron experiment reveals a sizable suppression of magnetic moment due to the superconductivity, indicating a possible phase coexistence. Here we propose that the observed suppression of the magnetic moment may be explained by the proximity effect within a phase-separation scenario. We use a two-orbital model to study the proximity effect on a layer of the block AFM state induced by neighboring SC layers via an interlayer tunneling mechanism. We argue that the proximity effect in ternary Fe selenides should be large because of the large interlayer coupling and weak electron correlation. The result of our mean-field theory is compared with the neutron experiments semiquantitatively. The suppression of the magnetic moment due to the SC proximity effect is found to be more pronounced in d-wave superconductivity and may be enhanced by the frustrated structure of the block AFM state.

DOI: 10.1103/PhysRevB.85.104506 PACS number(s): 74.20.Mn, 74.25.Ha, 74.62.En, 74.25.nj

I. INTRODUCTION

The recent discovery of high-T_c superconductivity in the ternary iron selenides $A_yFe_{2-x}Se_2$ (A = K, Rb, Cs, ...)[1–3] has triggered a new surge of interest in the study of iron-based superconductors (Fe-SCs). The fascinating aspect of this class of materials lies in the tunable Fe vacancies, which substantially modify the normal-state metallic behavior and enhance the transition temperature T_c to above 30 K from 9 K for the binary system FeSe at ambient pressure.[1,3,4] Particular attention has been focused on the vacancy ordered compound $K_{0.8}Fe_{1.6}Se_2$, or the so-called 245 system, as it introduces a novel magnetic structure into the already rich magnetism of an Fe-SC. Unlike the collinear[5–7] or bicollinear[8–10] AFM order observed in the parent compounds of other Fe-SCs, the neutron diffraction experiment has clearly shown that these materials have a block AFM (BAFM) order.[11] Meanwhile, the AFM order with an unprecedentedly large magnetic moment of $3.31\mu_B$/Fe below the Néel temperature is the largest one among all the known parent compounds of Fe-SCs.[11,12] Moreover, the carrier concentration is extremely low, indicating the parent compound to be a magnetic insulator or semiconductor,[13,14] in contrast to the metallic spin-density-wave (SDW) state of the parent compound in other Fe-SCs.[3,15]

The relation between the novel magnetism and superconductivity in ternary Fe selenides is currently an interesting issue under debate. The question is whether the superconductivity and the BAFM order are phase separated or coexist in certain regions of the phase diagram. The neutron experiment shows the suppression of the AFM ordering below SC transition point,[11] suggesting the coexistence. Some other experiments, such as two-magnon Raman scattering[16] and muon-spin rotation and relaxation,[17] are consistent with this picture. On the other hand, the ARPES[18] NMR[19] and TEM[20] experiments indicate a mesoscopic phase separation between the superconductivity and the insulating AFM state. Most recently, Li *et al*. showed the superconductivity and the BAFM orders to occur at different layers of the Fe-selenide planes in the STM measurement.[21]

The vacancy in Fe selenides is an interesting but complicated issue. The vacancy in the Fe selenide carries a negative charge since the Fe ion has a valence of 2+. In equilibrium, we expect the vacancies to repel each other at short distance for the Coulomb interaction and to attract to each other at a long distance for the elastic strain. Such a scenario would be in favor of phase separation to form vacancy-rich and vacancy-poor regions in the compound. The challenge is then to explain the observed suppression of the magnetic moment of the BAFM due to superconductivity. At the phenomenological level, the suppression of magnetism due to superconductivity has been reported previously,[22] and such a phenomenon may be explained by Ginzburg-Landau theory.[23]

In this paper, we propose that the proximity effect of superconductivity to the BAFM in mesoscopically phase-separated Fe selenides may be large to account for the suppression of the AFM moments observed in the neutron experiment. More specifically, we use a microscopic model to study the proximity effect on a layer of the BAFM state induced by an adjacent SC layer. The proximity effect in Fe selenides is expected to be important for the two reasons. One is the weaker correlation effect, and the other is the larger interlayer hopping amplitude, compared with those in cuprates. Both of them may enhance the proximity effect on the magnetism from the neighboring SC layer. Our model calculations show that the proximity effect in a mesoscopically phase-separated state of Fe selenides may explain various seemingly conflicted experiments.

II. MODEL AND MEAN-FIELD THEORY

$A_yFe_{2-x}Se_2$ is a layered material with FeSe layers separated by alkali-metal atoms, similar to the 122 material in the iron pnictides family. To investigate the proximity effect on the

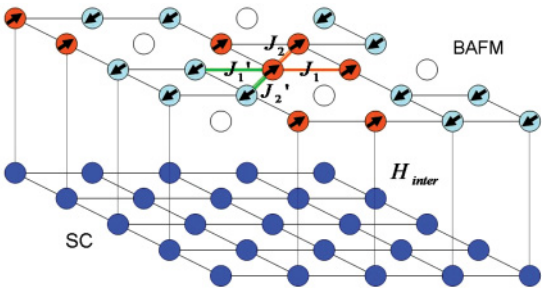

FIG. 1. (Color online) Schematic diagram of the system in our model to study proximity effect to the block AFM state (upper layer) induced by superconductivity at the lower layer via a pair tunneling process H_{inter} in Eq. (3).

BAFM layer, we consider a single BAFM layer next to a SC layer as shown schematically in Fig. 1. The electronic Hamiltonian describing the BAFM layer is given by

$$H = H_0 + H_{\text{inter}}, \tag{1}$$

where H_0 describes the electron motion and spin couplings in the BAFM layer and H_{inter} describes the coupling to the neighboring SC layer. We consider a two-orbital model to describe H_0,

$$\begin{aligned} H_0 = & -\sum_{ij,\alpha\beta,\sigma} t_{ij,\alpha\beta} C^\dagger_{i,\alpha\sigma} C_{j,\beta\sigma} - \mu \sum_{i,\alpha\sigma} C^\dagger_{i,\alpha\sigma} C_{i,\alpha\sigma} \\ & + J_1 \sum_{\langle ij\rangle,\alpha\beta} \mathbf{S}_{i,\alpha}\cdot\mathbf{S}_{j,\beta} + J_2 \sum_{\langle\langle ij\rangle\rangle,\alpha\beta} \mathbf{S}_{i,\alpha}\cdot\mathbf{S}_{j,\beta} \\ & + J_1' \sum_{\langle ij\rangle',\alpha\beta} \mathbf{S}_{i,\alpha}\cdot\mathbf{S}_{j,\beta} + J_2' \sum_{\langle\langle ij\rangle\rangle',\alpha\beta} \mathbf{S}_{i,\alpha}\cdot\mathbf{S}_{j,\beta}, \end{aligned} \tag{2}$$

where $C_{i,\alpha\sigma}$ annihilates an electron at site i with orbital α (d_{xz} and d_{yz}) and spin σ, μ is the chemical potential, $t_{ij,\alpha\beta}$ are the hopping integrals, and $\langle ij\rangle$ ($\langle ij\rangle'$) and $\langle\langle ij\rangle\rangle$ ($\langle\langle ij\rangle\rangle'$) denote the intrablock (interblock) nearest neighbor (NN) and next nearest neighbor (NNN) bonds, respectively (see the upper layer in Fig. 1). J_1 (J_2) are the exchange coupling constants for NN (NNN) spins in the same block, and J_1' (J_2') are for the two NN (NNN) spins in different blocks. The two-orbital model is a crude approximation for electronic structure. However, it may be a minimal model to capture some of basic physics in examining the proximity effect. The band structure around the obtained Fermi energy from the two-orbital model is shown in Fig. 2, which is very similar to the result obtained in density functional theory. The main shortcoming in using the two-orbital model is that the magnetic moment is 2 μ_B at its largest, smaller than the experimentally measured $3.31\mu_B$. We consider this to be a quantitative issue, and it will not qualitatively change our results.

We now consider H_{inter}, the coupling between the SC and BAFM layers. H_{inter} may be derived from an interlayer hopping Hamiltonian

$$H_c = \sum_{i,\alpha\beta,\sigma} t_{\tau,\alpha\beta} C^\dagger_{i,\alpha,\sigma} C^B_{i,\beta,\sigma} + \text{H.c.},$$

with the superscript B indicating the corresponding operator in the neighboring SC layer. Here we have assumed a nonzero hopping integral between the two sites on top of each other

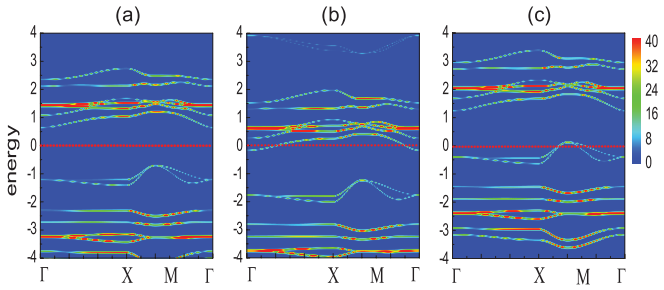

FIG. 2. (Color online) Electronic band structures of the mean-field decoupled H_0 given by Eq. (2). The parameters are given at the end of Sec. II of the text, and $J_1 = 2.0$. (a) At half filling or $n = 2.0$; (b) at electron doping $n = 2.1$; and (c) at hole doping $n = 1.9$. The color scale indicates the relative spectra weight.

in Fig. 1, consistent with the crystal structure.[21] Note that the vacancy site is excluded in the BAFM layer. Since we are interested in the proximity effect of the superconductivity to the neighboring BAFM layer, the effective pairing coupling on the BAFM layer is given, to second order in terms of the interlayer hopping $t_{\tau,\alpha\beta}$,

$$H_{\text{inter}} = \frac{t_\tau^2}{\omega_c} \sum_{ij,\alpha\beta,\alpha'\beta',\sigma} (C^\dagger_{i,\alpha,\sigma} C^B_{i,\beta,\sigma} C^\dagger_{j,\alpha',\bar\sigma} C^B_{j,\beta',\bar\sigma} + \text{H.c.}), \tag{3}$$

where $\omega_c \sim t_1$ is a characteristic energy, and we have assumed an orbital-independent interlayer hopping integral $t_\tau = t_{\tau,\alpha\beta}$ for simplicity. Note that a similar interlayer pair coupling Hamiltonian has been derived previously.[24,25] In Eq. (3) we have neglected all other nonpairing terms induced by the hopping Hamiltonian at the second order in $t_{\tau,\alpha\beta}$. In an Fe-SC, the interlayer hopping integral may be relatively large, so high-order corrections to the perturbation may not be negligible in a more quantitative study. However, we expect the basic physics is captured by the second-order pair tunneling term in Eq. (3).

With the mean-field approximation $\Delta_{ij,\alpha\alpha',\sigma\bar\sigma} = \langle C^B_{i,\alpha,\sigma} C^B_{j,\alpha',\bar\sigma}\rangle$, we have

$$H_{\text{inter}} = \sum_{ij,\beta\beta',\sigma} (V_{\tau,ij} C^\dagger_{i,\beta,\sigma} C^\dagger_{j,\beta',\bar\sigma} + \text{H.c.}), \tag{4}$$

where $V_{\tau,ij} = \frac{t_\tau^2}{\omega_c} \sum_{\alpha\alpha'} \Delta_{ij,\alpha\alpha',\sigma\bar\sigma}$.

The $\sqrt{5}\times\sqrt{5}$ vacancy order and the BAFM order lead to an enlarged unit cell with eight sites per unit cell. We use a mean-field theory for the Ising spins in Eq. (2) and obtain the Bogoliubov-de Gennes equations in the enlarged unit cell:

$$\begin{aligned} & {\sum_k}' \sum_{j,\beta} \begin{pmatrix} H_{ij,\alpha\beta,\sigma} + \tilde H_{ij,\alpha\beta,\sigma} & H_{c,ij,\alpha\beta} \\ H^*_{c,ij,\alpha\beta} & -H^*_{ij,\alpha\beta,\bar\sigma} + \tilde H_{ij,\alpha\beta,\sigma} \end{pmatrix} \\ & \times \exp[i\mathbf{k}\cdot(\mathbf{r}_j - \mathbf{r}_i)] \begin{pmatrix} u^k_{n,j,\beta,\sigma} \\ v^k_{n,j,\beta,\bar\sigma} \end{pmatrix} = E^k_n \begin{pmatrix} u^k_{n,i,\alpha,\sigma} \\ v^k_{n,i,\alpha,\bar\sigma} \end{pmatrix}, \end{aligned} \tag{5}$$

where the summations of k are over the reduced Brillouin zone, and

$$\begin{aligned} H_{ij,\alpha\beta,\sigma} &= -t_{ij,\alpha\beta} - \mu, \\ \tilde{H}_{ij,\alpha\beta,\sigma} &= \sum_{\tau} (J_{\tau,\text{intra}} + J_{\tau,\text{inter}}) \langle S_{i+\tau,\beta} \rangle \delta_{ij}, \\ H_{c,ij,\alpha\beta} &= V_{\tau,ij}. \end{aligned} \tag{6}$$

Here $J_{\tau,\text{intra}} = J_1$ ($J_{\tau,\text{inter}} = J_1'$) if $\tau = \pm\hat{x}, \pm\hat{y}$ and $J_{\tau,\text{intra}} = J_2$ ($J_{\tau,\text{inter}} = J_2'$) if $\tau = \pm\hat{x} \pm \hat{y}$. $\hat{x}$ and $\hat{y}$ denote the unit vectors along x and y directions, respectively. $\langle S_{i+\tau,\beta} \rangle$ is defined as $(n_{i+\tau,\beta,\uparrow} - n_{i+\tau,\beta,\downarrow})/2$, and $u^k_{n,j,\alpha,\sigma}$ ($u^k_{n,j,\beta,\bar{\sigma}}$), $v^k_{n,j,\alpha,\sigma}$ ($v^k_{n,j,\beta,\bar{\sigma}}$) are the Bogoliubov quasiparticle amplitudes on the jth site with corresponding eigenvalues E^k_n. The self-consistent equations of the mean fields are

$$\begin{aligned} n_{i,\beta,\uparrow} &= \sum_{k,n} \left| u^k_{n,i,\beta,\uparrow} \right|^2 f\left(E^k_n\right), \\ n_{i,\beta,\downarrow} &= \sum_{k,n} \left| v^k_{n,i,\beta,\downarrow} \right|^2 \left[1 - f\left(E^k_n\right)\right]. \end{aligned} \tag{7}$$

The magnitude of the magnetic order on the ith site and the induced SC pairing correlation in the BAFM layer are defined as

$$\begin{aligned} M(i) &= \frac{1}{2} \sum_{\beta} (n_{i,\beta,\uparrow} - n_{i,\beta,\downarrow}), \\ \Delta^A_{ij,\alpha\beta} &= \frac{1}{4} \sum_{k,n}{}' \left(u^k_{n,i,\alpha,\sigma} v^{k*}_{n,j,\beta,\bar{\sigma}} e^{-i\mathbf{k}\cdot(\mathbf{r}_j - \mathbf{r}_i)} \right. \\ &\quad \left. + v^{k*}_{n,i,\alpha,\bar{\sigma}} u^k_{n,j,\beta,\sigma} e^{i\mathbf{k}\cdot(\mathbf{r}_j - \mathbf{r}_i)} \right) \tanh\left(\frac{E^k_n}{2k_B T} \right). \end{aligned} \tag{8}$$

In the calculations, we choose the hopping integrals as follows.[26] Along the y direction, the $d_{xz} - d_{xz}$ NN hopping integral is $t_1 = 0.4$ eV and the $d_{yz} - d_{yz}$ NN hopping integral is $t_2 = 0.13$ eV; they are exchanged in the x direction; the NN interorbital hoppings are zero; the NNN intraorbital hopping integral is $t_3 = -0.25$ eV for both d_{xz} and d_{yz} orbitals, and the NNN interorbital hopping is $t_4 = 0.07$ eV. The hopping integral t_1 is taken as the energy unit. We keep $J_1 : J_1' : J_2 : J_2' = -4 : -1 : 1 : 2$.[27,28] The doping level is given by $\delta = n - 2.0$.

III. RESULTS

To begin with, we present the energy band structure of the self-consistently stabilized BAFM state of the mean-field decoupled H_0 at half filling with $n = 2$ in Fig. 2(a), where $J_1 = 2.0$ is so chosen to obtain a band gap ~500 meV in agreement with the first-principle calculations.[27,29] For the electron doping with $n = 2.1$, the Fermi level crosses an energy band around the center of the Brillouin zone [Γ point in Fig. 2(b)], while it intersects with an energy band around the zone corner at the hole doping with $n = 1.9$ [M point in Fig. 2(c)]. Although a simple two-orbital model is adopted here, both the electron and hole doping cases with $\delta = 0.1$ are qualitatively consistent with the first-principle calculations.[29] In the presence of the ordered vacancies and BAFM order, the original two-band structures are splitting into 16 subbands as a result of the enlarged unit cell with eight sites. At half filling, eight lower bands are occupied, i.e., 1/4 electron per one subband, while another eight bands above the Fermi energy are unoccupied, resulting in a band gap in Fig. 2. For the electron and hole doping with $\delta = 0.1$, the chemical potential crosses one subband, which produces the characteristic features of the Fermi surface and the metallic BAFM state.

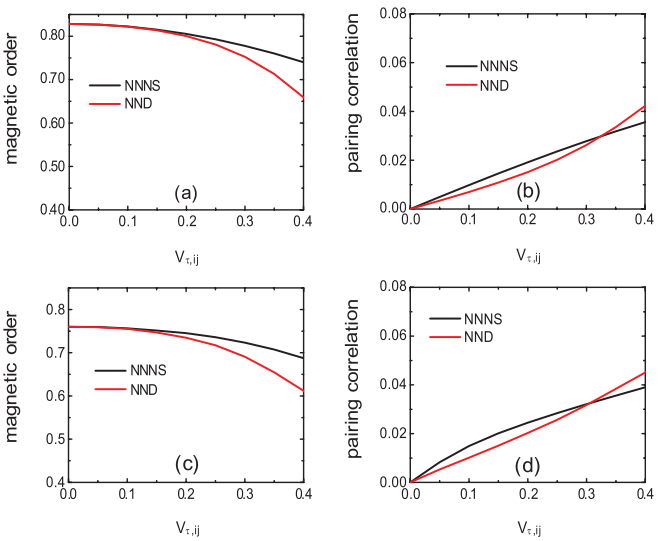

FIG. 3. (Color online) Block AFM moment and SC pairing correlation as functions of the effective tunneling strength $V_{\tau,ij}$. Black curves are for NNN $s_{\pm}$-wave pairing, and red (gray) for NN d-wave pairing. Panels (a) and (b): $n = 2.0$; (c) and (d): $n = 2.1$.

Motivated by the agreement of the self-consistent mean-field solutions with the mentioned first-principle calculations, we consider now the proximity effect in the BAFM layer induced by the superconductivity in the neighboring layer. We choose two possible spin singlet pairing symmetries on the SC layer, i.e., the NNN $s_{\pm}$-wave and the NN d-wave symmetries with their respective gap functions $\Delta_{s_{\pm}} = \Delta_0 \cos(k_x) \cos(k_y)$ and $\Delta_d = \Delta_0[\cos(k_x) - \cos(k_y)]$, where the former results in the NNN bond and the latter the NN bond couplings in the BAFM layer. The interlayer hopping constant t_τ is assumed to be site independent. Figure 3 displays the moment of the BAFM order as a function of the effective tunneling strength $V_{\tau,ij}$. At the half filling, for both $s_{\pm}$- and d-wave pairings, the interlayer coupling suppresses the magnetic order and induces the SC correlation in the BAFM layer. However, the suppression of the BAFM order is more pronounced when the neighboring layer has a d-wave pairing, as we can see from Figs. 3(a) and 3(b). At the electron doping with $n = 2.1$, the ground state in the absence of the interlayer coupling is a metallic BAFM state. The suppression of the BAFM order and the induced paring correlation due to the proximity effect are plotted in Figs. 3(c) and 3(d). They are qualitatively similar to the half-filled case of $n = 2$, possibly due to the very low total carrier concentration.

It will be interesting to compare our calculations with the neutron experiment, where the the magnetic order is found to be suppressed by the SC transition. For this purpose, we model the temperature-dependent SC pairing parameter by a BCS-like phenomenological form $\Delta(T) = \Delta_0\sqrt{1 - T/T_c}$ in our mean-field theory. We present the temperature dependence

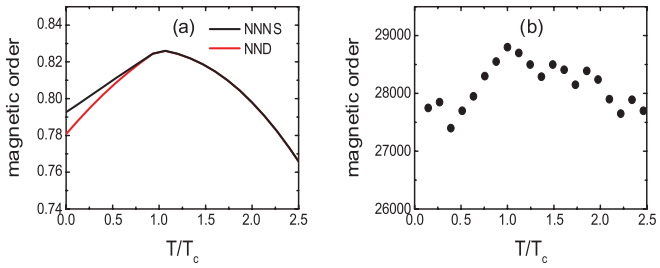

FIG. 4. (Color online) (a) Temperature dependence of the block AFM moment at $n = 2.0$. Black and red curves are for NNN $s_{\pm}$-wave and NN d-wave pair couplings, respectively. (b) The replotted curve of the neutron data from Ref. 11.

of the magnetic moment in Fig. 4(a) for a choice of the coupling constant $V_{\tau,ij}(T = 0) = 2t_{\tau}^2\Delta_0/\omega_c = 0.25$. As temperature decreases, the magnetic order increases when temperature is above T_c, while it decreases when temperature is below T_c, resulting in a broad peak around T_c. We note that the temperature dependence of the AFM moment is reminiscent of the neutron diffraction and two-magnon experiments [Fig. 4(b)].[11,16] There is another scenario in which the competition between the AFM and the SC orders in their microscopic coexistence may also produce the decrease of the AFM moment below T_c. The study of such a possibility is currently under way and the results will be published elsewhere. It is worthwhile to note that the sizable proximity effect relies on the substantial interlayer hopping constant t_{τ}. Based on the first-principle calculation, the interlayer hopping t_{τ} was estimated to have a comparable magnitude with t_1 possibly because of the high values of electron mobility from the intercalated alkaline atoms,[30] and this leads to the highly three-dimensional Fermi surface.[27,29]

IV. SUMMARY AND DISCUSSIONS

In summary, we have proposed that various seemingly conflicting experiments on the phase separation or coexistence of superconductivity and BAFM may be explained within a phase-separation scenario by taking into account of the proximity effect of superconductivity on the neighboring layer of BAFM. We have used a pair tunneling Hamiltonian to study the proximity effect on a BAFM layer induced by an adjacent SC layer in a simplified two-orbital model for Fe selenides. The proximity effect in reducing the moment of the BAFM order highly depends on the coupling constant $V_{\tau,ij}$. Our calculation shows that the superconductivity proximity effect may result in substantial suppression of the magnetic moment in Fe selenides. This is in contrary to that in the cuprate superconductor, where the coupling constant $V_{\tau,ij}$ is very small because of a small c-axis hopping integral due to the large anisotropy, and because of the renormalization of $V_{\tau,ij}$ by a factor proportional to the hole concentrations due to the no double-occupation condition.[31] In an iron-based superconductor, the anisotropy of iron-based material is much smaller than in the cuprate, which leads to a relatively larger t_{τ}. And the moderate correlation effect in an iron-based superconductor leads to a moderate renormalization factor. As a consequence, the coupling constant $V_{\tau,ij}$ in the iron chalcogenide superconductor should be moderate.

We remark that we would be careful in drawing a concrete conclusion to compare with the experiments. Our model is a much simplified theory. The approximation that only d_{xz} and d_{yz} orbitals are important in the bands close to the Fermi energy is good in terms of the band structures.[27,29] But the maximum magnetic moment in a two-orbital model is only 2 μ_B, smaller than the moment of $3.31\mu_B$ measured in experiments.[11,12] Also, we only calculated the suppression of the BAFM order of the surface layer of the BAFM domain. According to a TEM experiment,[20] each BAFM domain has around ten layers. And the suppression of the BAFM order of the layers in the middle of domain may be more complicated. Furthermore, the interlayer pair tunneling Hamiltonian (3) is derived from the interlayer hopping term from the perturbation theory at the second order in the hopping integral. For the relatively large interlayer hopping, the high-order contributions may not be negligibly small, and Eq. (3) may be a semiquantitative approximation only. In brief, the suppression of the BAFM moment is sizable because of the moderate coupling constant $V_{\tau,ij}$, and our calculation may be viewed as a semiquantitative result.

We also investigated the proximity effect for various pairing symmetry of the SC phase. It has been shown that the SC pairing with NN d-wave symmetry resulted in a more pronounced proximity effect in reducing the moment of the BAFM order than the NNN $s_{\pm}$-wave pairing. The second-order process induced proximity effect has a temperature dependence as the SC pairing, which may be relevant to the experimental observations. A more remarkable proximity effect was found in the BAFM state than in the conventional AFM state, which was a consequence of the frustrated structure and the associated anisotropic exchange interactions.

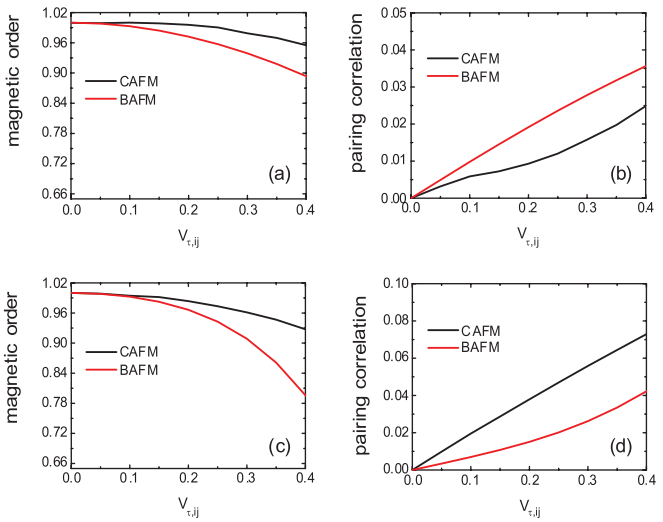

FIG. 5. (Color online) Comparison of the proximity effect between the block and conventional AFM states. Left column shows the moment of the AFM order, and right column the SC pairing correlation as functions of the effective tunneling strength $V_{\tau,ij}$. Panels (a) and (b): for the NNN $s_{\pm}$-wave pairing; (c) and (d): for the NN d-wave pairing.

ACKNOWLEDGMENTS

We thank W. Bao, G. Aeppli, Y. Zhou, and T. M. Rice for helpful discussions. This work is supported in part by Hong Kong's RGC GRF HKU706809 and HKUST3/CRF/09. H.M.J. is grateful to the NSFC (Grant No. 10904062), Hangzhou Normal University (HSKQ0043, HNUEYT), and the NSF of Zhejiang Province (No. Z6110033).

APPENDIX

In this Appendix, we compare the proximity effect in the BAFM state with that in the single-band conventional AFM (CAFM) system. We choose the dispersion $\varepsilon_k = -2t[\cos(k_x) + \cos(k_y)] - 4t' \cos(k_x)\cos(k_y) - \mu$ with $t = t_1$ and $t' = t_3$, which gives rise to the similar energy band width with that in the above two-orbital model and is close to the case of the cuprates. The AFM order is introduced by the AFM exchange interaction $J \sum_{\langle ij \rangle} \mathbf{S}_i \cdot \mathbf{S}_j$ between the NN sites. At the half filling $n = 1$, we find that $J = 1.6$ produces the comparable band gap and the electron polarization as in the above BAFM state. In Fig. 5, we present the magnitude of the magnetic order and the induced pairing correlation as a function of the effective tunneling $V_{\tau,ij}$. The upper panel shows the results for the NNN $s_\pm$-wave pairing and the lower panel the results for the NN d-wave pairing. In the figure, the magnitude of the magnetic order in both cases is renormalized. The proximity effect in reducing the AFM order is more pronounced for the BAFM state as shown in Figs. 5(a) and 5(c). As for the induced pairing correlation, the larger correlation is found in the BAFM state for the $s_\pm$-wave paring and in the CAFM state for the d-wave pairing, as displayed in Figs. 5(b) and 5(d), respectively.

We can understand the above results by considering the different spin configurations of the BAFM and CAFM orders, as shown in Fig. 6. In the BAFM state, when two electrons transfer from the BAFM layer to the SC one, the energy changes due to the bonds breaking for the NN bond coupling

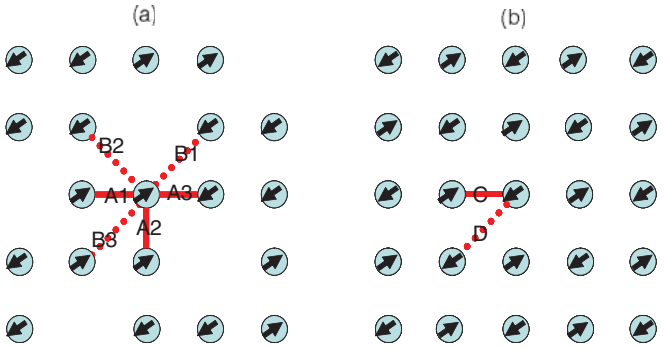

FIG. 6. (Color online) Comparison of the spin structures and their respective NN and NNN bonds. (a) Block AFM state; (b) conventional AFM state.

are $\Delta E_{\mathrm{NN}}^{\uparrow\uparrow} = |J_1|$ [A1 and A2 bonds in Fig. 6(a)] and $\Delta E_{\mathrm{NN}}^{\uparrow\downarrow} = 7|J_1|/4$ [A3 bond in Fig. 6(a)] for the electron pairs with ferromagnetic and antiferromagnetic alignments, respectively. On the other hand, the energy changes due the bonds breaking for the NNN bond are $\Delta E_{\mathrm{NNN}}^{\uparrow\uparrow} = 9|J_1|/4$ [B3 bond in Fig. 6(a)] and $\Delta E_{\mathrm{NNN}}^{\uparrow\downarrow} = 5|J_1|/2$ [B1 and B2 bonds in Fig. 6(a)]. The tunneling process occurs more easily when the energy cost due to the bonds breaking is small, so the proximity effect in reducing the moment of the AFM order by the d-wave pairing is more remarkable than that by the $s_\pm$ one. However, the energy changes due to the bonds breaking in the CAFM state are $\Delta E_{\mathrm{NN}} = 7|J|$ [C bond in Fig. 6(b)] and $\Delta E_{\mathrm{NNN}} = 8|J|$ [D bond in Fig. 6(b)] for the NN and NNN band couplings. Therefore, the proximity effect in reducing the moment of the AFM in the CAFM state is rather weak for both the $s_\pm$- and d-wave pairing couplings. As for the induced pairing correlation, the extent of the match between the AFM order configuration and the singlet SC pairing largely determines the magnitude of the induced pairing correlation. For example, the CAFM matches well with the NN d-wave pairing, so one can expect a large induced pairing correlation without the severe decrease of the AFM order, as displayed in Figs. 5(c) and 5(d).

[1] J. Guo, S. Jin, G. Wang, S. Wang, K. Zhu, T. Zhou, M. He, and X. Chen, Phys. Rev. B **82**, 180520(R) (2010).

[2] A. Krzton-Maziopa, Z. Shermadini, E. Pomjakushina, V. Pomjakushin, M. Bendele, A. Amato, R. Khasanov, H. Luetkens, and K. Conder, J. Phys. Condens. Matter **23**, 052203 (2011).

[3] M. H. Fang, H. D. Wang, C. H. Dong, Z. J. Li, C. M. Feng, J. Chen, and H. Q. Yuan, Europhys. Lett. **94**, 27009 (2011).

[4] Y. Zhang, L. X. Yang, M. Xu, Z. R. Ye, F. Chen, C. He, H. C. Xu, J. Jiang, B. P. Xie, J. J. Ying, X. F. Wang, X. H. Chen, J. P. Hu, M. Matsunami, S. Kimura, and D. L. Feng, Nat. Mater. **10**, 273 (2011).

[5] C. de la Cruz, Q. Huang, J. W. Lynn, J. Li, W. Ratcliff II, J. L. Zarestky, H. A. Mook, G. F. Chen, J. L. Luo, N. L. Wang, and P. Dai, Nature (London) **453**, 899 (2008).

[6] F. Ma, Z. Y. Lu, and T. Xiang, Phys. Rev. B **78**, 224517 (2008); Front. Phys. China **5**, 150 (2010).

[7] X. W. Yan, M. Gao, Z. Y. Lu, and T. Xiang, Phys. Rev. Lett. **106**, 087005 (2011).

[8] F. Ma, W. Ji, J. Hu, Z. Y. Lu, and T. Xiang, Phys. Rev. Lett. **102**, 177003 (2009).

[9] W. Bao, Y. Qiu, Q. Huang, M. A. Green, P. Zajdel, M. R. Fitzsimmons, M. Zhernenkov, S. Chang, M. Fang, B. Qian, E. K. Vehstedt, J. Yang, H. M. Pham, L. Spinu, and Z. Q. Mao, Phys. Rev. Lett. **102**, 247001 (2009).

[10] S. Li, C. de la Cruz, Q. Huang, Y. Chen, J. W. Lynn, J. Hu, Y. L. Huang, F. C. Hsu, K. W. Yeh, M. K. Wu, and P. Dai, Phys. Rev. B **79**, 054503 (2009).

[11] W. Bao, Q. Huang, G. F. Chen, M. A. Green, D. M. Wang, J. B. He, X. Q. Wang, and Y. Qiu, Chin. Phys. Lett. **28**, 086104 (2011).

[12] Z. Shermadini, A. Krzton-Maziopa, M. Bendele, R. Khasanov, H. Luetkens, K. Conder, E. Pomjakushina, S. Weyeneth, V. Pomjakushin, O. Bossen, and A. Amato, Phys. Rev. Lett. **106**, 117602 (2011).

[13] Y. Zhou, D.-H. Xu, F.-C. Zhang, and W.-Q. Chen, Europhys. Lett. **95**, 17003 (2011).
[14] R. Yu, J.-X. Zhu, and Q. Si, Phys. Rev. Lett. **106**, 186401 (2011).
[15] R. H. Yuan, T. Dong, Y. J. Song, P. Zheng, G. F. Chen, J. P. Hu, J. Q. Li, and N. L. Wang, Sci. Rep. **2**, 221 (2012).
[16] A. M. Zhang, J. H. Xiao, Y. S. Li, J. B. He, D. M. Wang, G. F. Chen, B. Normand, Q. M. Zhang, and T. Xiang, e-print arXiv:1106.2706.
[17] Z. Shermadini, A. Krzton-Maziopa, M. Bendele, R. Khasanov, H. Luetkens, K. Conder, E. Pomjakushina, S. Weyeneth, V. Pomjakushin, O. Bossen, and A. Amato, Phys. Rev. Lett. **106**, 117602 (2011).
[18] F. Chen, M. Xu, Q. Q. Ge, Y. Zhang, Z. R. Ye, L. X. Yang, J. Jiang, B. P. Xie, R. C. Che, M. Zhang, A. F. Wang, X. H. Chen, D. W. Shen, J. P. Hu, and D. L. Feng, Phys. Rev. X **1**, 021020 (2011).
[19] D. A. Torchetti, M. Fu, D. C. Christensen, K. J. Nelson, T. Imai, H. C. Lei, and C. Petrovic, Phys. Rev. B **83**, 104508 (2011).
[20] Z. Wang, Y. J. Song, H. L. Shi, Z. W. Wang, Z. Chen, H. F. Tian, G. F. Chen, J. G. Guo, H. X. Yang, and J. Q. Li, Phys. Rev. B **83**, 140505(R) (2011).
[21] W. Li, H. Ding, P. Deng, K. Chang, C. Song, K. He, L. Wang, X. Ma, J.-P. Hu, X. Chen, and Q.-K. Xue, Nat. Phys. **8**, 126 (2012).
[22] G. Aeppli, D. Bishop, C. Broholm, E. Bucher, K. Siemensmeyer, M. Steiner, and N. Stusser, Phys. Rev. Lett. **63**, 676 (1989).
[23] E. I. Blount, C. M. Varma, and G. Aeppli, Phys. Rev. Lett. **64**, 3074 (1990).
[24] S. Chakravarty, A. Sudbø, P. W. Anderson, and S. Strong, Science **261**, 337 (1993).
[25] W. L. McMillan, Phys. Rev. **175**, 537 (1968).
[26] W.-G. Yin, C.-C. Lee, and W. Ku, Phys. Rev. Lett. **105**, 107004 (2010).
[27] C. Cao and J. Dai, Phys. Rev. Lett. **107**, 056401 (2011).
[28] Y.-Z. You, H. Yao, and D.-H. Lee, Phys. Rev. B **84**, 020406(R) (2011).
[29] X.-W. Yan, M. Gao, Z.-Y. Lu, and T. Xiang, Phys. Rev. B **83**, 233205 (2011).
[30] C. Cao (private communication).
[31] M. Mori, T. Tohyama, and S. Maekawa, J. Phys. Soc. Jpn. **75**, 034708 (2006).